ISBN: 978-3-95450-214-1 ISSN: 2673-5490 doi:10.18429/JACoW-IPAC2021-THPAB060

DISPERSION CONTROLLED TEMPORAL SHAPING OF PHOTOINJECTOR LASER PULSES FOR ELECTRON EMITTANCE REDUCTION IN X-RAY FREE ELECTRON LASERS

R. Lemons *[1], N. Neveu, J. Duris, A. Marinelli, S. Carbajo
SLAC National Accelerator Laboratory, Menlo Park, CA, USA
C. Durfee, Colorado School of Mines, Illinois, CO, USA
[1]also at Colorado School of Mines, Illinois, CO, USA

Abstract

Temporal shaping of photocathode excitation laser pulses is a long-sought-after challenge to tailor the phase-space of electrons. The temporal profile of lasers, typically upconverted from infrared to ultraviolet, have significant impact on the distribution and time-evolution of the collective electron bunches. Towards this end, we present a method combining efficient nonlinear upconversion with simultaneous and adaptable temporal profile shaping through dispersion-controlled sum-frequency generation resulting in temporal profiles with sharp rise-fall times and flat top profiles. Using the LCLS-II photoinjector as a case study, we demonstrate a reduction in generated electron transverse emittance by upwards of 30% over conventionally implemented temporal profiles. Additionally, we discuss the ongoing experimental implementation of this method and preliminary results.

INTRODUCTION

In photoinjectors, electrons are generated via the photoelectric effect with laser pulses comprised of light above the work function of the material. During emission, the temporal intensity profile of the laser pulse can significantly effect electron bunch quality. A key measure of quality is the transverse emittance, ϵ_x, defined as [1]

$$\epsilon_x = \sqrt{\langle x_i^2 \rangle \langle x_i'^2 \rangle - \langle x_i^2 x_i'^2 \rangle}, \quad (1)$$

where x is transverse position and x' is the corresponding angle with respect to the ideal trajectory. In XFELs, in addition to low emittance (< 1.5 µm), it is particularly crucial to have electron bunches with narrow energy spread ($\Delta E/E < 10^{-3}$) and good spatial uniformity, as growth in these parameters can significantly decrease x-ray production in the undulators [2]. Though electron quality and energy spread can be improved through the use of spatio-temporally shaped IR lasers in laser heaters [3–5], a more broadly applicable and foundational approach is to shape the existing photoexcitation laser to generate higher quality electron bunches from the beginning. Conventionally implemented photoexcitation laser profiles are Gaussian in time though other commonly sought-after laser distributions are shown to reduce transverse emittance such as flat-top spatio-temporal profiles resembling cylinders [6] or 3D ellipsoids such that the beam size and intensity vary as a function of time [7].

* rlemons@slac.stanford.edu

Realizing these non-Gaussian profiles is achieved through either spectral or temporal techniques. Spectral methods, such as spatial-light modulators [8] or acousto-optic modulators [9], suffer from distortion during pulse amplification and upconversion, limited spectral bandwidth, and by material damage threshold limitations [10]. On the other hand, intensity fluctuations inherent to temporal techniques based on pulse stacking [11], have been shown to induce unwanted microbunching [12, 13] on the electron bunch, resulting in increased emittance relative to Gaussian distributions. In order to operate at the correct wavelength, these lasers also typically employ a series of nonlinear conversion stages to upconvert infrared (IR) light to UV light below 270 nm [14, 15]. Efficient optical upconversion, necessary for electron production, is detrimentally affected by non-zero phase structure and can distort temporal profiles, complicating shaping efforts. As such, these methods are limited in their applicability to high average power, 24/7 facilities, such as LCLS.

We present a technique blending shaping and nonlinear conversion thereby circumventing the pitfalls of existing upconversion and shaping techniques [16]. By combining non-colinear sum frequency generation (Fig. 1) with two highly dispersed pulses we generate a pulse with tunable temporal profile in duration and shape. We expand on Raoult *et al.* [17] of efficient narrowband second harmonic generation in thick crystals by adding third-order dispersion to simultaneously shape the output pulse. The resultant pulse can be directly upconverted to UV without distortion. This method, which we call dispersion controlled nonlinear shaping (DCNS), can be broadly used to tailor pulses for the reduction of normalized transverse emittance in photoinjector-based instrumentation.

PHOTOEXCITATION SIMULATION

The electric field of a laser pulse in frequency space is given by $E(\omega) = A(\omega)e^{i\varphi(\omega)}$ where $A(\omega)$ is the spectral amplitude, typically modeled as a Gaussian distribution around the central frequency, and $\varphi(\omega)$ is the spectral phase. We define $\varphi(\omega)$ via a Taylor expansion about the central frequency,

$$\varphi(\omega) = \varphi_0 + \varphi_1(\omega - \omega_0) + \frac{\varphi_2}{2!}(\omega - \omega_0)^2 + \frac{\varphi_3}{3!}(\omega - \omega_0)^3 + \frac{\varphi_4}{4!}(\omega - \omega_0)^4 + \ldots, \quad (2)$$

ISBN: 978-3-95450-214-1 ISSN: 2673-5490 doi:10.18429/JACoW-IPAC2021-THPAB060

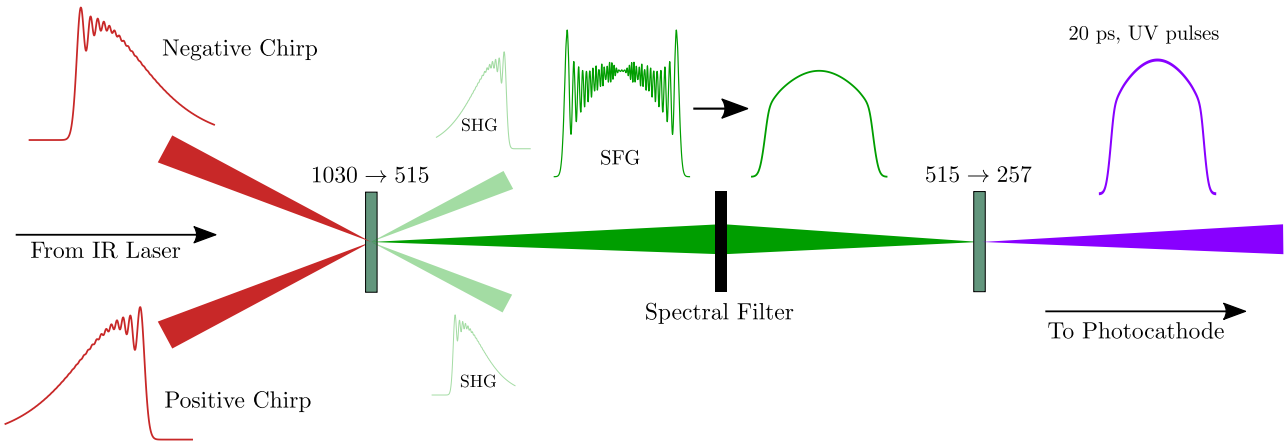

Figure 1: Schematic diagram of the DCNS method being used to generate a temporally flattened UV pulse from equal and oppositely dispersed infrared pulses. The spectral filter included between the two upconversion stages serves to eliminate unwanted oscillations on the edges of the optical pulse.

where φ_j is the j^{th} derivative of $\varphi(\omega)$ evaluated at ω_0. Dropping the first two terms, which are arbitrary for our purposes, we focus on the next two terms, second order dispersion (SOD), φ_2, and third order dispersion (TOD), φ_3. SOD is a linear instantaneous temporal chirp on the pulse primarily effecting duration while TOD is quadratic instantaneous chirp creating temporal oscillations on either the leading or falling edge of the pulse. Additionally, we define the ratio $\alpha = \varphi_3/\varphi_2$ (s) allowing us to set pulse duration with SOD and change shape with α.

To evaluate these pulses, and their electron generation, compared to the baseline Gaussian pulses, we simulate the photoinjector system at LCLS-II. The laser system consists of a 1030 nm, 50 µJ, 330 fs commercial laser with an approximately 4 nm full width at half maximum (FWHM) spectral bandwidth. To generate a flattened profile, we focus on situations where α is near to 0.125 ps. The initial value of SOD (≈ 3.5 ps^2) was chosen so that the FWHM of the laser pulse would be 25 ps in time [15].

The resultant pulse after the first conversion stage from 1030 nm to 515 nm (Fig. 2a) displays a sharp rise time and flatter profile than the traditionally used Gaussian pulses; however, it also displays large and rapid amplitude fluctuations on the picosecond scale that can be detrimental to e-beam emittance. By applying a spectral amplitude filter (Fig. 2b), the high frequency components can be attenuated and the temporal profile flattened. The UV laser pulse is then generated from this filtered profile.

We then simulate the LCLS-II photoinjector system with these profiles and a Gaussian of equivalent FWHM. The simulation code used for e-beam dynamics is OPAL [18], and for particle distribution generation, distgen [19]. While supplying the DCNS pulses is straightforward, determining the optimal FWHM and spot size on the cathode is not. The strength of the space charge forces are directly impacted by both the FWHM and spot size, which then impacts how strong the external forces need to be to limit emittance growth. To determine optimal laser and machine settings,

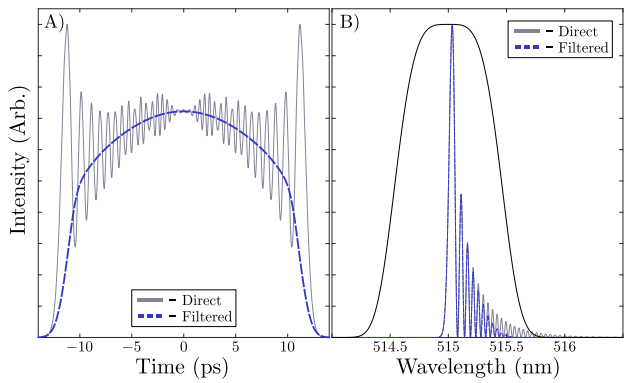

Figure 2: Optimal 515 nm laser profile for a bunch length of 1.22 mm resulting in an emittance value of 0.30 µm. The two plots shown are, a) the laser profile in time before (grey) and after (blue, dashed) a 0.5 nm spectral filter, and b) the spectrum of the pulse before (grey) and after filtering (blue, dashed) with the super-gaussian spectral filter in black.

the simulation is run in combination with an optimization algorithm (NSGA-II [20]).

To maintain broad applicability of these results, we limit the simulation to only the photoinjector and the first 15 meters of acceleration ($\approx$ 100 MeV), after which are LCLS-II specific configurations. This also serves to limit the simulation to a region where space-charge forces are not yet damped by highly relativistic speeds and the effect of the laser is prominent.

The metrics commonly used for determining beam quality for XFELs are emittance (1) and bunch length (σ_z). Note, we do not optimize the orthogonal transverse dimension, y, because the simulation is transversely symmetric. Several optimization rounds were performed to compare the performance of DCNS and Gaussian laser pulses in the LCLS-II photoinjector. Final results are shown in Figs. 3 and 4, with the later showing density of simulation points near the Pareto fronts.

ISBN: 978-3-95450-214-1 ISSN: 2673-5490 doi:10.18429/JACoW-IPAC2021-THPAB060

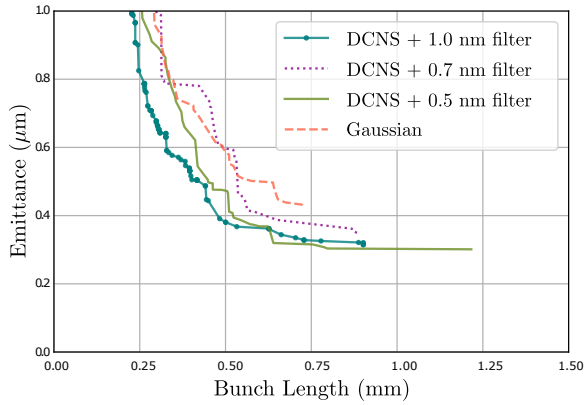

Figure 3: Pareto front comparison of DCNS and Gaussian performance for the LCLS-II injector. DCNS pulses in combination with a 1.0 nm spectral filter achieves the lowest emittance values at most bunch lengths. The absolute lowest achieved emittance value is 0.30 µm at a bunch length of 1.22 mm, using a 0.5 nm filter.

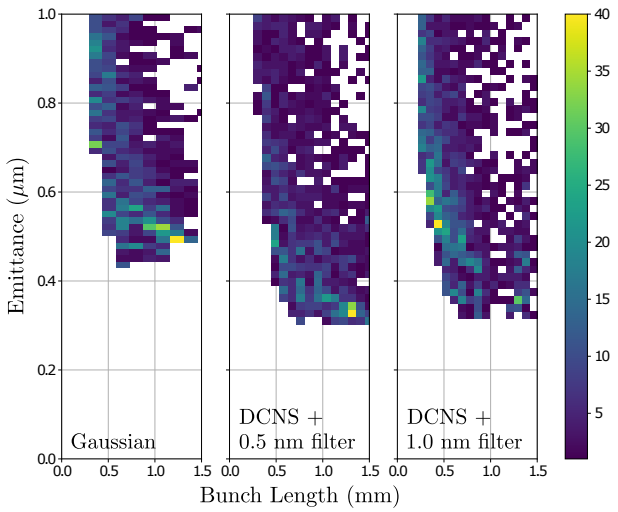

Figure 4: Histogram showing simulation density of all GA solutions, not only Pareto optimal, for Gaussian and DCNS cases. Lighter colored areas indicate a higher number of simulations with valid solutions and thus regions where different methods might be more effective.

As shown in Fig. 3, the best value found is $\epsilon_x = 0.30\,\mu m$ with the the DCNS pulse shown in Fig. 2. The bunch length in this case, 1.22 mm, is slightly longer than the typical operating length of 1 mm at LCLS. For a practical comparison, we choose the minimum emittance values at $\sigma_z = 1$ mm. A 25% improvement in the emittance value is obtained from DCNS ($\epsilon_x = 0.37\,\mu m$) vs. Gaussian ($\epsilon_x = 0.50\,\mu m$) pulses. Note, this Gaussian point is not visible in Fig. 3, because it is not Pareto optimal. For shorter bunch lengths, i.e. 0.5 mm, the difference is slightly larger reaching about 30% ($\epsilon_x = 0.4\,\mu m$ vs $0.58\,\mu m$). Applying this reduction to both x and y planes, since the simulation is symmetric, the total transverse brightness can be more than doubled. In the case of XFELs, this emittance improvement translates to a twofold increase in undulator peak brightness, 25% shorter x-ray wavelengths, and an upper bound reduction in undulator lengths by 25% for similar peak currents, which can substantially reduce cost, complexity, and size.

CONCLUSION

Electron emittance, and by extension the electron beam brightness, can be improved through temporal tailoring of the photoinjector drive laser, enabling further exploration of research areas backed by electron photoinjectors. Existing shaping techniques for the excitation lasers suffer from challenges in maintaining pulse shapes, providing sufficient photon throughput, or even increasing electron emittance, as can be the case with pulse-stackers. DCNS circumvents these issues by directly upconverting optical pulses and embedding favorable temporal distributions in the sum frequency conversion using highly dispersed pulses. In the case of linear accelerators and XFELs such the LCLS-II, this simple solution is expected to improve electron emittance across all investigated bunch lengths over conventional Gaussian pulses with an upwards of 30% emittance reduction at short bunch lengths (0.25 mm) and 25% at bunch lengths greater than or equal to 1 mm. This method stands as a realistic avenue to substantially extend the brightness of photoinjector systems worldwide without major configuration changes and thus enhance current scientific capabilities on existing accelerators and reduce the cost of future accelerator facilities.

ACKNOWLEDGEMENTS

We thank Yuantao Ding and Christopher Mayes at SLAC National Accelerator Laboratory for their helpful discussions.

This work is supported by the U.S. Department of Energy, Office of Science, Office of Basic Energy Sciences under Contract No. DE-AC02-76SF00515.

REFERENCES

[1] H. Wiedemann, "Particle beams and phase space", in *Particle Accelerator Physics*, Switzerland: Springer International Publishing, 2015, pp. 213–251.

[2] Z. Huang and K.-J. Kim, "Review of x-ray free-electron laser theory", *Phys. Rev. ST Accel. Beams*, vol. 10, p. 034801, Mar. 2007. doi:10.1103/PhysRevSTAB.10.034801

[3] Z. Huang *et al.*, "Suppression of Microbunching Instability in the Linac Coherent Light Source", *Physical Review Special Topics-Accelerators and Beams*, vol. 7, no. 7, p. 074401, 2004. doi:10.2172/826776

[4] N. Liebster *et al.*, "Laguerre-gaussian and beamlet array as second generation laser heater profiles", *Physical Review Accelerators and Beams*, vol. 21, no. 9, p. 090701, 2018. doi:10.1103/physrevaccelbeams.21.090701

[5] J. Tang *et al.*, "Laguerre-gaussian mode laser heater for microbunching instability suppression in free-electron lasers", *Physical Review Letters*, vol. 124, no. 13, p. 134 801, 2020. doi:10.1103/physrevlett.124.134801

ISBN: 978-3-95450-214-1 ISSN: 2673-5490 doi:10.18429/JACoW-IPAC2021-THPAB060

[6] M. Krasilnikov *et al.*, "Experimentally minimized beam emittance from an l-band photoinjector", *Physical Review Special Topics-Accelerators and Beams*, vol. 15, no. 10, p. 100701, 2012. doi:10.1103/physrevstab.15.100701

[7] O. Luiten, S. Van der Geer, M. De Loos, F. Kiewiet, and M. Van Der Wiel, "How to realize uniform three-dimensional ellipsoidal electron bunches", *Physical review letters*, vol. 93, no. 9, p. 094 802, 2004. doi:10.1103/physrevstab.15.100701

[8] S. Y. Mironov *et al.*, "Shaping of cylindrical and 3d ellipsoidal beams for electron photoinjector laser drivers", *Applied optics*, vol. 55, no. 7, pp. 1630–1635, 2016. doi:10.1364/ao.55.001630

[9] Y. Li, S. Chemerisov, J. Lewellen, *et al.*, "Laser pulse shaping for generating uniform three-dimensional ellipsoidal electron beams", *Physical Review Special Topics-Accelerators and Beams*, vol. 12, no. 2, p. 020702, 2009. doi:10.1103/physrevstab.12.020702

[10] S. Carbajo and K. Bauchert,"Power handling for LCoS spatial light modulators", *Laser Resonators, Microresonators, and Beam Control XX*, vol. 10518, p. 105181R 2018. doi:10.1117/12.2288516

[11] M. Krasilnikov, Y. Chen, and F. Stephan, "Studies of space charge dominated electron photoemission at pitz", *Journal of Physics: Conference Series*, vol. 1238, 2019, p. 012064. doi:10.1088/1742-6596/1238/1/012064

[12] S. Bettoni *et al.*, "Impact of laser stacking and photocathode materials on microbunching instability in photoinjectors", *Phys. Rev. Accel. Beams*, vol. 23, p. 024401, Feb. 2020. doi:10.1103/PhysRevAccelBeams.23.024401

[13] C. E. Mitchell, J. Qiang, M. Venturini, and P. Emma, "Sensitivity of the Microbunching Instability to Irregularities in Cathode Current in the LCLS-II Beam Delivery System", in *Proc. North American Particle Accelerator Conf. (NAPAC'16)*, Chicago, IL, USA, Oct. 2016, pp. 1171–1173. doi:10.18429/JACoW-NAPAC2016-THPOA32

[14] I. Will, H. I. Templin, S. Schreiber, and W. Sandner, "Photoinjector drive laser of the flash fel", *Optics Express*, vol. 19, no. 24, pp. 23770–23781, 2011. doi:10.1364/oe.19.023770

[15] S. Gilevich *et al.*, "The lcls-ii photo-injector drive laser system", in *Proc. 2020 Conference on Lasers and Electro-Optics (CLEO'20)*, San Jose, CA, USA, May 2020, pp. 1–2.

[16] R. Lemons, N. Neveu, J. Duris, A. Marinelli, C. Durfee, and S. Carbajo, "Dispersion-controlled temporal shaping of picosecond pulses via non-colinear sum frequency generation", 2020. arXiv:2012.00957

[17] F. Raoult *et al.*, "Efficient generation of narrow-bandwidth picosecond pulses by frequency doubling of femtosecond chirped pulses", *Optics letters*, vol. 23, no. 14, pp. 1117–1119, 1998. doi:10.1364/ol.23.001117

[18] A. Adelmann *et al.*, "Opal a versatile tool for charged particle accelerator simulations", 2019. arXiv:1905.06654

[19] C. Gulliford, DistGen: Particle distribution generator, https://github.com/ColwynGulliford/distgen

[20] K. Deb, A. Pratap, S. Agarwal, and T. Meyarivan, "A fast and elitist multiobjective genetic algorithm: NSGA-II", *IEEE Trans. Evol. Comp.*, vol. 6, no. 2, pp. 182–197, Apr. 2002. doi:10.1109/4235.996017